

Effect of FSP Pass Number on the Tribological Behavior of AZ31 Magnesium Alloy

M.M. Jalilvand, Y. Mazaheri*, A.R. Jahani

Materials Engineering Department, Bu-Ali Sina University, Hamedan, Iran.

Article info

Article history:

Received 04 September 2019

Received in revised form

16 November 2019

Accepted 28 December 2019

Keywords:

Friction stir processing (FSP)

Grain refinement

AZ31 magnesium alloy

Microhardness wear

Friction

Abstract

Friction stir processing (FSP) in different pass number, accordingly one and four, was performed to AZ31 magnesium alloy. Optical and scanning electron microscopy (SEM) were used to investigate the effect of FSP and its pass number on the microstructure of FSPed samples. The hardness of the samples was measured using microhardness measurement. Furthermore, wear behaviors of the samples, including wear rate and friction coefficient, were investigated using a reciprocal wear machine. To deduce the wear mechanism, SEM observations of the worn surface were carried out. Optical microscopy of FSPed samples showed grain refinement in the stir zone. Increasing FSP pass number had a considerable effect on grain refinement. The average grain size of the as-received AZ31 base metal reduced from $11\mu\text{m}$ to about $4\mu\text{m}$ after four passes. Microhardness evaluations showed a substantial improvement by increasing FSP pass number, about 70% improvement. Wear tests results revealed enhanced tribological in FSPed samples. SEM observations of the worn surfaces indicated that the abrasion was the dominant wear mechanism governed in the samples.

1. Introduction

One of the important design parameters is weight-saving constituents in structural applications. Mg and its alloys are the most attractive materials for the structural component such as automotive and aerospace equipment because of being the lightest structural metallic materials [1]. However, usage of these alloys is still limited because of the mechanical properties and corrosion resistance are not fit to the desired level [2]. For rectification of these properties, a few solutions such as adjusting the microstructure of alloys by a suitable choice of alloying elements, optimizing their processing, and refinement of the microstructure have been proposed [3-5]. In practice, the surface properties, e.g., wear resistance of a component determines its lifetime. Then, one solution is to refine the surface

layer of a constituent.

So far, various techniques in which the operating temperature is high and material transform to the liquids state, have been employed to modify the surface of alloys such as laser surface engineering [6], irradiation by high-energy electron beam [7], thermal spraying [8], cast sinter [9], GTA treatment [10]. The operating temperatures of these techniques are high, and usually, the material transforms to the liquids state.

Performing the surface treatment in the liquid state suffers some problems including, the occurrence of detrimental reactions between the matrix and reinforcement and also phase transformations. For this matter, it is favorable to carry out these techniques in the solid-state [11].

One of the solid-state processing of the surfaces

*Corresponding author: Y. Mazaheri (Assistant Professor)

E-mail address: y.mazaheri@basu.ac.ir

<http://dx.doi.org/10.22084/jrstan.2020.19994.1107>

ISSN: 2588-2597

is friction stir processing (FSP). This process was invented by Thomas et al. [12] at the Welding Institute (TWI). In these family processes, i.e. FSW and FSP, a microstructure evolution usually occurs in the stir zone [13]. This microstructure evolution in a controlled condition which can result in grain refinement in the stir zone leading to better properties. It could be proposed in the metallurgical point of view that FSP is a thermo-mechanical treatment which is capable of adjusting surface microstructure of metals and alloys [14]. This process has several advantages such as refined microstructure, homogeneity, solid-state processing, and environment-friendly and energy-efficient process. So, FSP is appropriate for several types of metal and alloys such as aluminum and magnesium alloys [13, 15].

There are several research papers on the FSP of AZ31 magnesium alloy which have dealt with the evolution of the microstructure [16–22]. Chang et al. [18] used FSP to produce nano grain structure in AZ31 Mg alloy. Zhang et al. [21] correlated the superplasticity of AZ31 magnesium alloy to the rotational tool speed and pin profile during FSP. Moreover, FSP was employed to improve the corrosion performance of the AZ series of magnesium alloys. Liu et al. [23] reported that the FSP can improve corrosion behavior of the AZ91 Mg alloy in 3.5 wt% NaCl aqueous solution, which is attributed to the enhanced passivity of the corrosion product film. According to the studies above, there are some criteria for selecting the pass number of FSP such as industrial limits, tool susceptibility and the quality of samples surfaces.

To the best knowledge of the authors, the effect of FSP pass numbers on the tribology behavior of AZ31 Mg alloy has not been dealt with in depth and needs to be considered in future research. The objective of this research is to investigate the effect of FSP pass number on the microstructural evolution, microhardness changes, and tribological properties i.e. wear and friction of the AZ31 Mg alloy.

2. Materials and Method

2.1. Materials

In this study, hot-rolled AZ31 bars of 10 mm thickness and $100 \times 50 \text{ mm}^2$ area, with the chemical analysis given in Table 1, were used for the FSP experiments.

2.2. Sample Processing

As is shown in Fig. 1, the sample is stabilized by some fixtures. During FSP, sample movement and vibration can deviate pin advancing from its original direction. Using fixtures hinders any sample displacing. To fabricate flawless samples by FSP, the process parameters

must be optimized. The presence of defects limits sample performance. Thus, different rotational and traverse tool velocities were tried. The optimum values of the traverse and rotational speeds are suggested to be 56 mm/min and 1000 rpm, respectively. Therefore, all of the samples were friction stir processed with the mentioned speeds and tool tilt angle of 2 degree clockwise. The tool used in the study was a threaded cylindrical pin with a shoulder. The dimension and picture of the tool are shown in Fig. 2.

Table 1

Chemical analyses of AZ31 bars.

Element	Mg	Al	Zn	Mn
Composition (wt. %)	Bal.	3.2	0.93	0.56

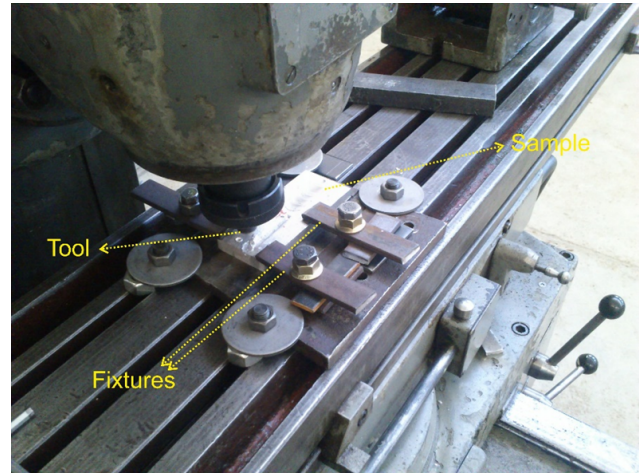


Fig. 1. Picture of the specimen fixtures and the FSP machine used in this study.

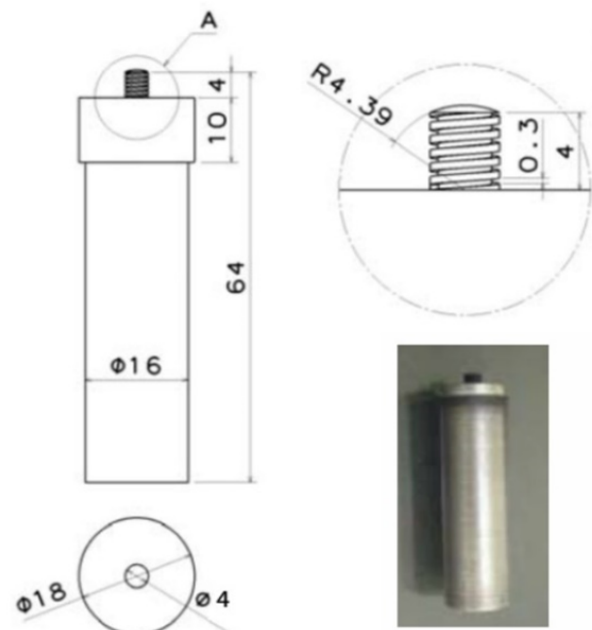


Fig. 2. Picture of the FSP tool with its dimensions (in mm).

2.3. Characterizations

To investigate the microstructure of the samples, metallographic practices, i.e. grinding, polishing and then etching with etchant made of 4.2g picric acid, 10ml acetic acid, 10ml distilled water and 70ml ethanol for 5 to 10 seconds were carried out [24]. The optical microstructures were captured using the Union optical microscope from the cross-sections of the samples.

The microstructural characterization and elemental composition of the base metal and friction stirred samples were analyzed using SEM (Jeol, 840JSM) equipped with an energy dispersive spectrometer (EDS) devices. Moreover, to determine the grain size of the different samples, the microstructural image processing (MIP) software version 4 was employed.

The microhardness measurements were done by the Buhler's equipment in the force of 100g for 15 seconds. The microhardness profile was obtained from the sample cross-section.

In order to investigate the tribological behavior of the specimens, a reciprocating wear machine was used. The pin was made of AISI 52100 steel with the hardness of 63HRC. The wear tests were carried out at the room temperature ($\sim 25^\circ\text{C}$) and humidity range of 30 to 50pct in unlubricated conditions. The sliding velocity, distance, and the applied load were 0.1m/s, 500m and 10N, respectively. These values were determined from pre conducted loadability tests. Mass losses of the specimens were measured at each 100m interval in sliding distance using the Mettler Toledo ME204 digital weight indicator with an accuracy of 0.1mg. The friction coefficients were continuously measured versus sliding distance. In order to verify the results, the friction-and-wear tests were determined by the average of three measurements. The SEM analyses of the worn surfaces were used to determine the wear mechanisms.

3. Results and Discussion

3.1. Parameter Optimizing

Several combinations of FSP parameters including traverse speed and tool rotation were examined to select the optimum condition. It is worth noting that the values of the parameters for examining and selecting the optimum conditions were chosen based on experiments carried out on AZ31 Mg alloy [16, 17, 25-29]; Moreover, it is worth mentioning that by increasing the traverse speed of the tool, the time length of the process would be less. Consequently, the growth of the grains is limited and the size of grains is lower [30]. Eventually, 1000rpm and 56mm/min were chosen as the optimum values for suitable traverse speed and tool rotation rate, respectively [31]. This combination conducted fabricating samples without any defects such as the tunnel, pinhole, piping, and wormhole with good

surface appearance (Fig. 3).

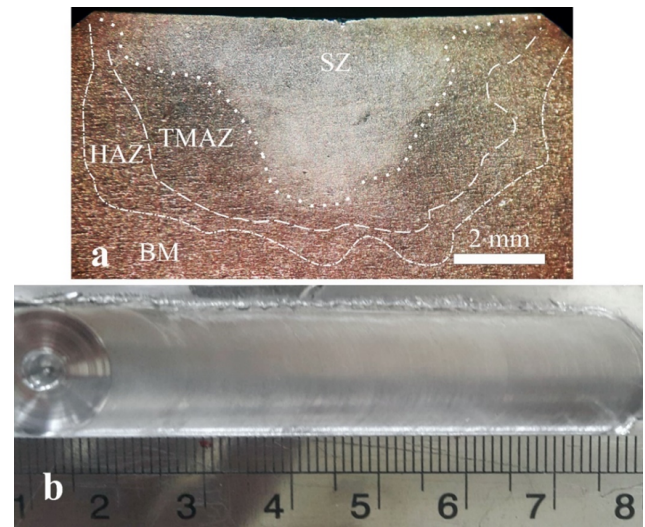


Fig. 3. a) Microstructure of FSPed AZ31 sample at cross-section view, and b) Surface of the sample after 1 pass.

3.2. Microstructural Evaluations

Fig. 4 illustrates the optical microstructures of the stir zone (SZ) of BM, 1-pass FSPed BM, and 4-pass FSPed BM samples. The microstructure of as-received AZ31 magnesium alloy consists of equiaxed grain with large and small sizes. Deformation twins were observed in the microstructure. Furthermore, there is a chance for the formation of the second phases and their distribution around the α -Mg grain boundaries [32].

In addition, SEM images taken from the SZ of the samples are shown in Fig. 5. It is obviously observed from Fig. 5 that by FSPing of the samples, the grain size decreased. Increasing pass number of FSP cause more reduction in grain size in 4-pass FSPed sample. Additionally, deformation twins were removed from the microstructure. During the FSP, the heat generated by friction and severe plastic deformation are simultaneously inducted into the processed material. This leads to the formation of dynamically recrystallized grains [33]. The typical recrystallization temperatures for Mg alloys were 0.5-0.7T_m. During FSP, the temperature of Mg alloys could reach the temperature range. Under the combined effect of high strain rate and elevated temperature, complete dynamic recrystallization and significant grain refinement were achieved in the FSPed AZ31 samples. As a result of that, the equiaxed grains can be formed [17].

Grain sizes of the samples were estimated using MIP software. These values are presented in Table 2. The values show that FSPing of the samples causes about 50% decrease in the average grain size. The occurrence of the dynamic recrystallization due to the continuous plastic deformation in the SZ is the reason

for this decrease [34]. The average grain size of the as-received AZ31 base metal reduced from about $11\mu\text{m}$ to about $4\mu\text{m}$ after four passes of FSP.

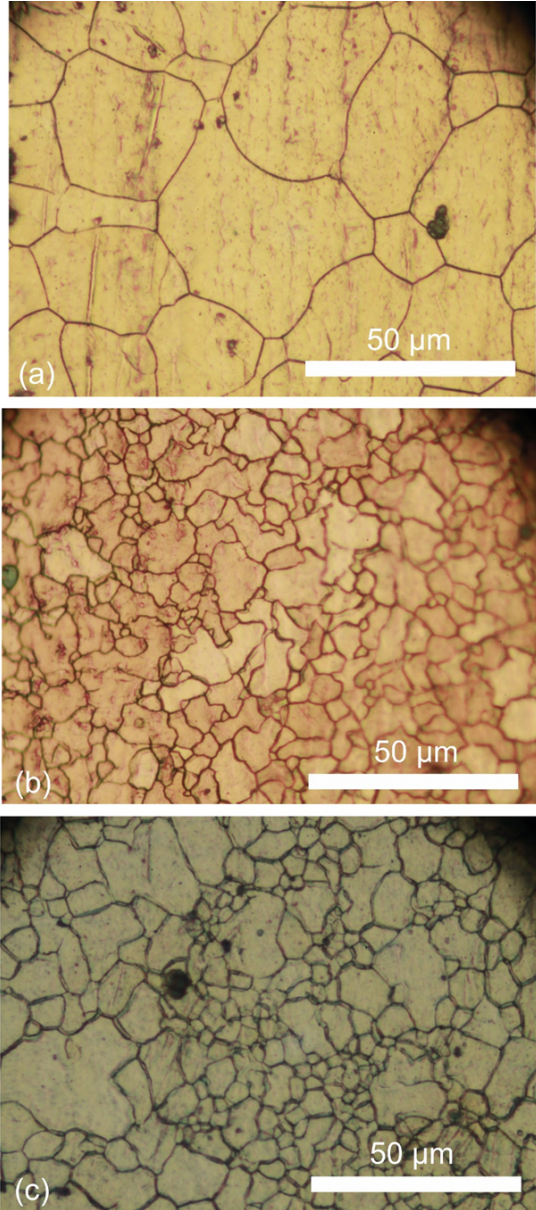


Fig. 4. Optical microstructures of the a) AZ31 base metal, b) 1-pass FSPed and c) 4-pass FSPed base metal.

Table 2

Average grain size of the samples.

Sample	Average grain size (μm)
BM	10.7 ± 2.1
1-PASS	5.3 ± 0.7
4-PASS	3.7 ± 0.5

3.3. Hardness

Table 3 presents the average hardness values and indentation prints obtained from the surface of the sam-

ples. The average of at least three measurements was reported as the surface hardness. The hardness of matrix and composites was also calculated using Eq. (1) [35]:

$$HV = 40 + 72d^{-1/2} \quad (1)$$

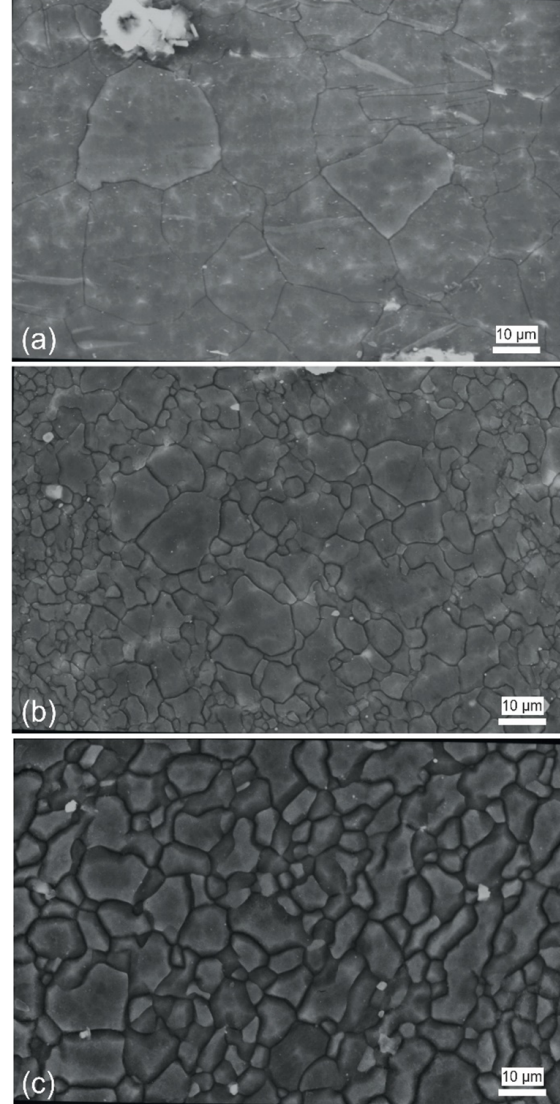
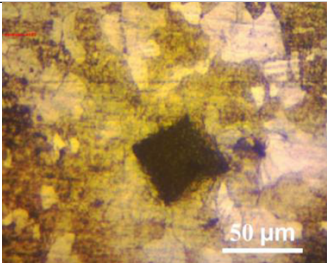
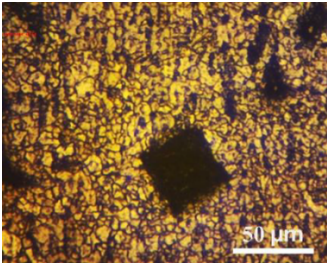
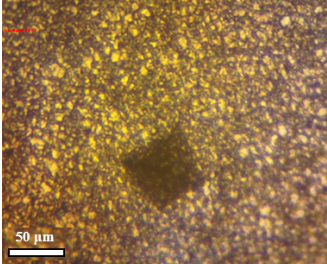


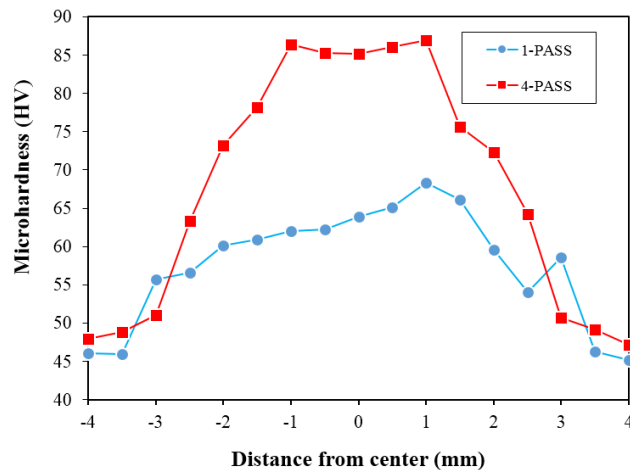
Fig. 5. SEM images of the a) AZ31 base metal, b) 1-pass FSPed, and c) 4-pass FSPed base metal.

In Eq. (1) d is the average grain size of the samples which was reported in Table 3. The cross-section microhardness profiles of the samples are shown in Fig. 6. The microhardness of the BM was about 45–49 HV. Significant improvements in the hardness were obtained as a result of FSP. Microhardness of AZ31 base alloy enhanced around 40% after one-pass FSP. Based on the Hall Petch equation, grain size refinement causes the hardness increase due to grain boundary strengthening [36]. According to this, smaller grains have higher microhardness values which match with the measured hardness values of FSPed BM sample. A further significant improvement occurred after four passes of FSP.

Table 3

The comparison between measured and calculated (Eq. (1)) microhardness of the samples with their indenter prints.

Sample	Measured microhardness (HV)	Calculated microhardness (HV)	Indenter prints
BM	48.6 ± 1.4	61.9	
1-Pass	59.5 ± 1.5	71.2	
4-Pass	85 ± 2	77.5	

**Fig. 6.** Microhardness profile taken from cross-section of the samples.

3.4. Wear Behavior

3.4.1. Wear Rate

Fig. 7 indicates the wear rate i.e., cumulative mass lost divided on sliding distance of the BM, 1-pass and 4-pass FSPed BM samples as a function of sliding distance at a sliding speed of 0.1m/s under normal force of 10N. Obviously, the wear rate of the AZ31 base metal is higher than other samples. By applying the FSP, the wear rate of the samples decreased slightly. Moreover,

by increasing passes of FSP, the wear rate reduced. Regarding the measured wear rates, the minimum wear rate belongs to the 4-pass FSPed sample.

As explained in the previous section, the increase in hardness values was attributed to the grain refinement occurred in the stir zone of FSPed samples. This directly affected on wear behaviors of Mg alloys with a major alloying element of Al, and as seen in the Fig. 7, decreases the wear rate [26, 37–39]. Based on Archard's equation, the wear rate relates inversely with hardness [40]:

$$Q = \frac{K.F.D}{H} \quad (2)$$

where Q is the worn volume per sliding distance, K is the wear coefficient, D is the sliding distance, F is the applied load, and H is the hardness of the worn surface. The measured wear rates and microhardness of the samples follow this equation. The major factors that contributed to the reduced wear rates for 4-pass NC sample could be attributed to the microstructural refinement which led into higher hardness, more work hardening capability, and enhanced ductility [29, 33].

3.4.2. Friction

Fig. 8 indicate the variations of the friction coefficient (FC) versus the sliding distance in the applied load of

10N for the BM, 1-pass and 4-pass FSPed BM samples. Moreover, average FC values for each sample were calculated. The base metal had the maximum FC average value (0.50), and the lowest values were obtained for 4-pass FSPed specimens, (0.27). Researchers [42] suggested that the coefficient of friction is related to the lubricant role of debris, the contact state, and area. Samples with higher hardness, have a lesser friction coefficient due to the fact that the harder surface usually involves a smaller contact area at a constant applied load [43].

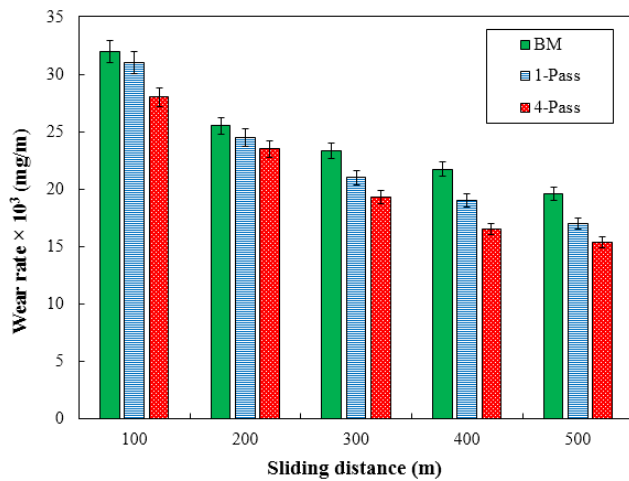


Fig. 7. Wear rate of the samples against sliding distance.

Researchers introduced friction as the force needed to overcome and break the bonding occurring due to local joining and adhesion in asperities at contact interfaces [44]. The FC of the samples reaches a steady state after a short running period due to the removal of adsorbed surface impurities [45]. Regarding Fig. 8, it can be seen that increasing sliding distance, the FC values of the BM, 1-pass and 4-pass FSPed BM samples become higher and also FC variation range of them become more extensive. Literature shows the increase in FC with the sliding distance is because of work-hardening phenomenon and accumulating of hard wear debris particles in the transfer layer [37, 46]. However, Mathis et al. [47] reported that in the case of AZ91D Mg alloy, the work-hardening phenomenon does not occur during friction and wear test. Thus, it seems this improvement is related to the formation and presence of hard debris. Besides, as reported by Mazaheri et al. [41] and Abbasi et al. [38], the high FC of BM at longer sliding distances is attributed to local welding of the worn debris to the sample surface which indicates domination of adhesive wear mechanism.

It can be seen that by increasing FSP pass number, the average friction coefficient becomes lower and its scattering reduces. In fact, a more homogenous microstructure was obtained in the 4-pass FSPed sample. Homogeneity of the alloy removes the large variation

in friction coefficient.

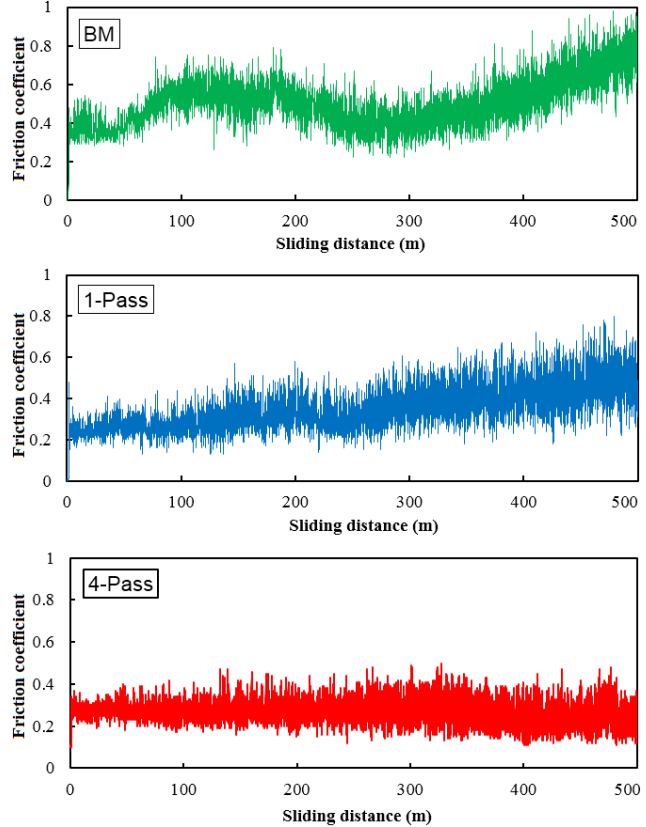


Fig. 8. The variations of friction coefficient as a function of sliding distance for the samples.

3.4.3. Wear Mechanism

Typically, several mechanisms play role in wearing a sample. In order to deduce the mechanisms involved in wear process of the samples, the worn surfaces of the counterface were investigated by SEM. Studies showed that in the wear regime map of the AZ31 Mg alloy abrasion and delamination wear mechanism are the typical mechanism at low sliding velocities and normal loads [48, 49]. Fig. 9 displays SEM micrograph of worn surfaces of the BM, 1-pass and 4-pass FSPed samples, the worn surface consists of delamination, micro-cutting, plowing, and grooves features. During reciprocating sliding of wear test, the repeated motion of the debris can generate subsurface cracks which initiate fatigue wear. Afterwhile, these cracks reach the surface and remove the metal in the form of laminates or sheet-like flakes debris and leave craters on the worn surface. This phenomenon is commonly known as delamination [29, 49].

The abrasive wear features such as micro-cutting, plowing, and grooves running parallel to the sliding direction are noticeable on the surfaces of FSPed BM, 1-pass, and 4-pass samples. Hard asperities on the steel counterface or hard fragments between the pin and surface cause wear by the removal of material from the substrate [50, 51].

By increasing the FSP pass number, the extent of these features was diminished. It should be noted that the 4-pass FSPed sample shows a better condition. In this case, delamination of the 4-pass sample is limited. The 4-pass FSPed sample has the lowest grain size, highest microhardness, and has seen the lowest wear rate among all. In fact, as mentioned above, the dominant wear mechanism for the FSPed BM, 1-pass and 4-pass samples is abrasive, and hardness plays an important role in abrasive wear. As shown, the 4-pass

sample had the highest hardness and lowest wear rate, which supported this idea.

Moreover, the SEM images of debris resulted from wearing of the samples after 500m are shown in Fig. 10. The platelike wear debris, as shown in Fig. 10a can indicate the delamination of the worn surfaces in the BM sample. From Fig. 10b, it is obvious that the size of these plate-like wear debris was reduced which indicated that delamination or abrasion occurred less intensively in the harder samples (FSPed samples).

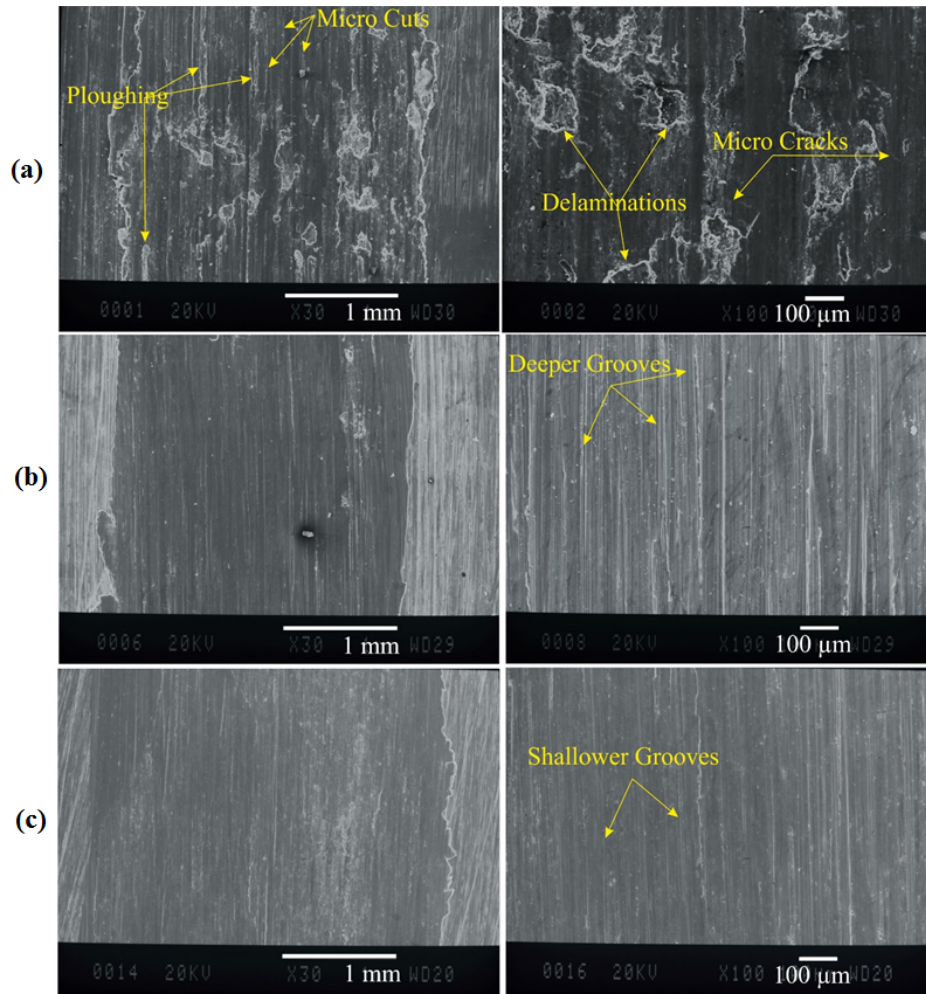


Fig. 9. SEM micrographs on worn surfaces of a) BM, b) 1-pass FSPed BM, c) 4-pass FSPed BM samples at different magnifications.

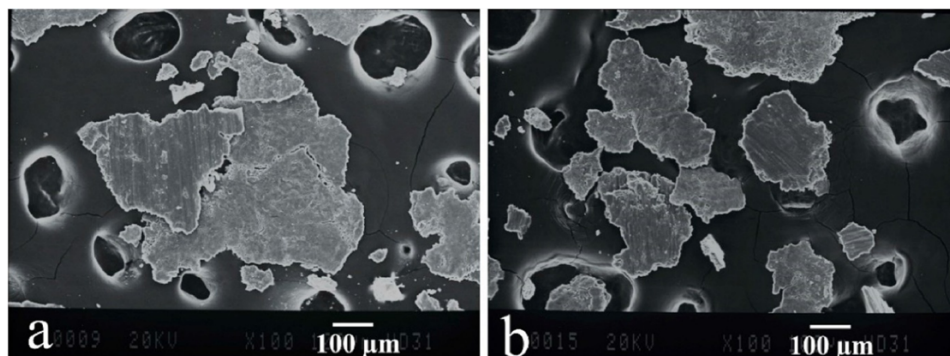


Fig. 10. SEM images of the debris resulting from wearing of the samples after 500m dry sliding wear test.

4. Conclusions

In this study, FSP was employed to treat the surface of AZ31 magnesium alloy in one- and four-pass cases. Examining of the microstructure and tribological behavior of the samples brings below conclusions:

1. Microstructural investigations indicated that FSP leads to significant grain refinement. By increasing pass number this refinement intensifies in such a way that after four passes of FSP, the average grain size of the sample decreased to about 4µm.
2. Microhardness measurements demonstrate 1-pass FSP causes little improvement in hardness; although by increasing the FSP pass number, hardness values of the sample increased significantly.
3. The wear rate of the four passes FSPed sample was minimum among the other samples which indicate improvement in the wear performance of the AZ31 base metal and 1-pass FSPed base metal.
4. The average friction coefficient was reduced from 0.5 for base metal to 0.27 for the 4-pass FSPed base metal.
5. SEM observation revealed that the abrasive wear mechanism occurred in the samples; however, the delamination of the surface was observed in the case of AZ31 base metal.

References

- [1] M. Avedesian, H. Baker, ASM specialty handbook: magnesium and magnesium alloys, ASM International Publisher, (1999).
- [2] M. Esmaily, J.E. Svensson, S. Fajardo, N. Birbilis, G.S. Frankel, S. Virtanen, R. Arrabal, S. Thomas, L.G. Johansson, Fundamentals and advances in magnesium alloy corrosion, *Prog. Mater. Sci.*, 89 (2017) 92-193.
- [3] P. Ian, J. David St, N. Jian-Feng, Q. Ma, *Light Alloys: Metallurgy of the Light Metals*, 5nd Edition, Elsevier Ltd, (2017).
- [4] N.S. Martynenko, E.A. Lukyanova, V.N. Serebryany, M.V. Gorshenkov, I.V. Shchetinin, G.I. Raab, S.V. Dobatkin, Y. Estrin, Increasing strength and ductility of magnesium alloy WE43 by equal-channel angular pressing, *Mater. Sci. Eng. A*, 712 (2018) 625-629.
- [5] Y. Zhang, F. Wang, J. Dong, L. Jin, C. Liu, W. Ding, Grain refinement and orientation of AZ31B magnesium alloy in hot flow forming under different thickness reductions, *J. Mater. Sci. Technol.*, 34(7) (2018) 1091-1102.
- [6] J. Dutta Majumdar, B. Ramesh Chandra, A.K. Nath, I. Manna, Compositionally graded SiC dispersed metal matrix composite coating on Al by laser surface engineering, *Mater. Sci. Eng. A*, 433(1-2) (2006) 241-250.
- [7] E. Yun, K. Lee, S. Lee, Correlation of microstructure with high-temperature hardness of (TiC, TiN)/Ti-6Al-4V surface composites fabricated by high-energy electron-beam irradiation, *Surf. Coat. Technol.*, 191(1) (2005) 83-89.
- [8] H.K. Kang, S.B. Kang, Thermal decomposition of silicon carbide in a plasma-sprayed Cu/SiC composite deposit, *Mater. Sci. Eng. A*, 428(1-2) (2006) 336-345.
- [9] Y. Wang, X. Zhang, G. Zeng, F. Li, Cast sinter technique for producing iron base surface composites, *Mater. Des.*, 21(5) (2000) 447-452.
- [10] W.B. Ding, H.Y. Jiang, X.Q. Zeng, D.H. Li, S.S. Yao, The surface modified composite layer formation with boron carbide particles on magnesium alloy surfaces through pulse gas tungsten arc treatment, *Appl. Surf. Sci.*, 253(8) (2007) 3877-3883.
- [11] N. Chawla, K.K. Chawla, *Metal Matrix Composites*, 2 Edition, Springer-Verlag, New York Publication, (2013).
- [12] W.M. Thomas, E.D. Nicholas, J.C. Needham, M.G. Murch, P. Templesmith, C.J. Dawes, International Patent Application No. PCT/GB92/02203 and GB Patent Application No. 9125978.8 (1991).
- [13] Z.Y. Ma, Friction stir processing technology: A review, *Metall. Mater. Trans. A*, 39(3) (2008) 642-658.
- [14] G.K. Padhy, C.S. Wu, S. Gao, Friction stir based welding and processing technologies - processes, parameters, microstructures and applications: A review, *J. Mater. Sci. Technol.*, 34(1) (2018) 1-38.
- [15] S.H. Nourbakhsh, A. Atrian, Effect of submerged multi-pass friction stir process on the mechanical and microstructural properties of Al7075, *J. Stress Anal.*, 2(1) (2017) 51-56.
- [16] V.V. Kondaiah, P. Pavanteja, P. Afzal Khan, S. Anand Kumar, R. Dumpala, B. Ratna Sunil, Microstructure, hardness and wear behavior of AZ31 Mg alloy - fly ash composites produced by friction stir processing, *Mater. Today: Proc.*, 4(6) (2017) 6671-6677.

- [17] B.M. Darras, M.K. Khraisheh, F.K. Abu-Farha, M.A. Omar, Friction stir processing of commercial AZ31 magnesium alloy, *J. Mater. Process. Technol.*, 191(1-3) (2007) 77-81.
- [18] C.I. Chang, X.H. Du, J.C. Huang, Producing nanograined microstructure in Mg–Al–Zn alloy by two-step friction stir processing, *Scr. Mater.*, 59(3) (2008) 356-359.
- [19] W. Wen, W. Kuaishe, G. Qiang, W. Nan, Effect of friction stir processing on microstructure and mechanical properties of cast AZ31 magnesium alloy, *Rare Met. Mater. Eng.*, 41(9) (2012) 1522-1526.
- [20] B. Darras, E. Kishta, Submerged friction stir processing of AZ31 Magnesium alloy, *Mater. Des.*, 47 (2013) 133-137.
- [21] D.T. Zhang, F. Xiong, W.W. Zhang, C. Qiu, W. Zhang, Superplasticity of AZ31 magnesium alloy prepared by friction stir processing, *Trans. Nonferrous Met. Soc. China*, 21(9) (2011) 1911-1916.
- [22] A. Alavi Nia, H. Omidvar, S.H. Nourbakhsh, Effects of an overlapping multi-pass friction stir process and rapid cooling on the mechanical properties and microstructure of AZ31 magnesium alloy, *Mater. Des.*, 58 (2014) 298-304.
- [23] Q. Liu, Q.X. Ma, G.Q. Chen, X. Cao, S. Zhang, J.L. Pan, G. Zhang, Q.Y. Shi, Enhanced corrosion resistance of AZ91 magnesium alloy through refinement and homogenization of surface microstructure by friction stir processing, *Corros. Sci.*, 138 (2018) 284-296.
- [24] American Society for Testing and Materials (Philadelphia, Pa.). ASTM E3-01: Standard Guide for Preparation of Metallographic Specimens. ASTM.
- [25] Y. Morisada, H. Fujii, T. Nagaoka, M. Fukusumi, Effect of friction stir processing with SiC particles on microstructure and hardness of AZ31, *Mater. Sci. Eng. A*, 433(1-2) (2006) 50-54.
- [26] D. Lu, Y. Jiang, R. Zhou, Wear performance of nano- Al_2O_3 particles and CNTs reinforced magnesium matrix composites by friction stir processing, *Wear*, 305(1-2) (2013) 286-290.
- [27] M. Balakrishnan, I. Dinaharan, R. Palanivel, R. Sivaprakasam, Synthesize of AZ31/TiC magnesium matrix composites using friction stir processing, *J. Magnes. Alloy.*, 3(1) (2015) 76-78.
- [28] M. Azizieh, A.H. Kokabi, P. Abachi, Effect of rotational speed and probe profile on microstructure and hardness of AZ31/ Al_2O_3 nanocomposites fabricated by friction stir processing, *Mater. Des.*, 32(4) (2011) 2034-2041.
- [29] C.I. Chang, Y.N. Wang, H.R. Pei, C.J. Lee, X.H. Du, J.C. Huang, Microstructure and mechanical properties of nano- ZrO_2 and nano- SiO_2 particulate reinforced AZ31-Mg based composites fabricated by friction stir processing, *Key Eng. Mater.*, 351 (2007) 114-119.
- [30] P. Asadi, G. Faraji, M.K. Besharati, Producing of AZ91/SiC composite by friction stir processing (FSP), *Int. J. Adv. Manuf. Technol.*, 51(1-4) (2010) 247-260.
- [31] Y. Mazaheri, M.M. Jalilvand, A. Heidarpour, A.R. Jahani, Tribological behavior of AZ31/ ZrO_2 surface nanocomposites developed by friction stir processing, *Tribol. Int.*, 143 (2020) 106062, doi.org/10.1016/j.triboint.2019.106062.
- [32] N.N. Aung, W. Zhou, Effect of grain size and twins on corrosion behaviour of AZ31B magnesium alloy, *Corros. Sci.*, 52(2) (2010) 589-594.
- [33] C.I. Chang, Y.N. Wang, H.R. Pei, C.J. Lee, J.C. Huang, On the hardening of friction stir processed Mg-AZ31 based composites with 5-20% nano- ZrO_2 and nano- SiO_2 particles, *Mater. Trans.*, 47(12) (2006) 2942-2949.
- [34] P. Asadi, G. Faraji, A. Masoumi, M.K. Besharati Givi, Experimental investigation of magnesium-base nanocomposite produced by friction stir processing: Effects of particle types and number of friction stir processing passes, *Metall. Mater. Trans. A*, 42(9) (2011) 2820-2832.
- [35] C.I. Chang, C.J. Lee, J.C. Huang, Relationship between grain size and Zener-Holloman parameter during friction stir processing in AZ31 Mg alloys, *Scr. Mater.*, 51(6) (2004) 509-514.
- [36] C.J. Lee, J.C. Huang, P.J. Hsieh, Mg based nanocomposites fabricated by friction stir processing, *Scr. Mater.*, 54(7) (2006) 1415-1420.
- [37] H.S. Arora, H. Singh, B.K. Dhindaw, Wear behaviour of a Mg alloy subjected to friction stir processing, *Wear*, 303(1-2) (2013) 65-77.
- [38] M. Abbasi, B. Bagheri, M. Dadaei, H.R. Omidvar, M. Rezaei, The effect of FSP on mechanical, tribological, and corrosion behavior of composite layer developed on magnesium AZ91 alloy surface, *Int. J. Adv. Manuf. Technol.*, 77(9-12) (2015) 2051-2058.
- [39] N. Singh, J. Singh, B. Singh, N. Singh, Wear behavior of B4C reinforced AZ91 matrix composite fabricated by FSP, *Mater. Today: Proc.*, 5(9) (2018) 19976-19984.
- [40] J.F. Archard, Contact and rubbing of flat surfaces, *J. Appl. Phys.*, 24(8) (1953) 981-988.

- [41] Y. Mazaheri, F. Karimzadeh, M.H. Enayati, Tribological Behavior of A356/ Al_2O_3 Surface Nanocomposite Prepared by Friction Stir Processing, *Metall. Mater. Trans. A*, 45(4) (2014) 2250-2259.
- [42] S.C. Lim, M.F. Ashby, Overview no. 55 Wear-mechanism maps, *Acta Metall.*, 35(1) (1987) 1-24.
- [43] H.Q. Sun, Y.N. Shi, M.X. Zhang, Wear behaviour of AZ91D magnesium alloy with a nanocrystalline surface layer, *Surf. Coat. Technol.*, 202(13) (2008) 2859-2864.
- [44] F.P. Bowden, D. Tabor, *The Friction and Lubrication of Solids*, 1st ed, Oxford University Press (OUP), (2001).
- [45] Y. Liu, B. Jin, D.J. Li, X.Q. Zeng, J. Lu, Wear behavior of nanocrystalline structured magnesium alloy induced by surface mechanical attrition treatment, *Surf. Coat. Technol.*, 261 (2015) 219-226.
- [46] Y.S. Zhang, Z. Han, K. Wang, K. Lu, Friction and wear behaviors of nanocrystalline surface layer of pure copper, *Wear*, 260(9-10) (2006) 942-948.
- [47] K. Máthis, Z. Trojanová, P. Lukáč, Hardening and softening in deformed magnesium alloys, *Mater. Sci. Eng. A*, 324(1-2) (2002) 141-144.
- [48] C. Liang, C. Li, X.X. Lv, J. An, Correlation between friction-induced microstructural evolution, strain hardening in subsurface and tribological properties of AZ31 magnesium alloy, *Wear*, 312(1-2) (2014) 29-39.
- [49] Q.B. Nguyen, Y.H. Sim, M. Gupta, C.Y.H. Lim, Tribology characteristics of magnesium alloy AZ31B and its composites, *Tribol. Int.*, 82 (2015) 464-471.
- [50] M. Shanthi, C.Y.H. Lim, L. Lu, Effects of grain size on the wear of recycled AZ91 Mg, *Tribol. Int.*, 40(2) (2007) 335-338.
- [51] A.D. Sarkar, *Wear of metals*. Pergamon Press, (1976).